Wideband Beamspace Massive MIMO Channel Estimation

Yang Nie

School of Physics and Electronic Information Engineering, Jining Normal University, Ulanqab 012000, China

Abstract: Millimeter-wave (mmWave) Massive multiple-input multiple-output (Massive MIMO) communication can provide high-speed network services for emerging application scenarios due to the abundant spectrum resources in the high-frequency band, which has emerged as a key technology for future wireless networks. Beamspace Massive MIMO systems equipped with lensed antenna arrays (LAA) have attracted considerable attention from industry and academic since it is an effective solution with low power and low cost. However, the beam squint effect causes beamspace channel estimation to be significantly complicated in wideband beamspace Massive MIMO systems. To address this problem, we investigate a channel estimator based on the vector approximate message passing (VAMP) algorithm to improve the estimation performance. Specifically, the wideband beamspace channel estimation is firstly considered as the two-dimensional (2D) image reconstruction problem. Subsequently, by the VAMP-based scheme, the 2D natural image is accurately sparse reconstructed from noisy linear measurements, which effectively solve the channel estimation problem. Simulation results verify the effectiveness of the proposed method and highlight its excellent performance in terms of the channel estimation.

Keywords: Massive MIMO; MMWave communication; Channel estimation; Beamspace; VAMP.

1. Introduction

Millimeter-wave (mmWave) communication has garnered significant attention in recent years since it can leverage the abundant spectral resources of high-frequency bands to achieve high-speed data rates [1,2]. With the explosion of high-resolution services and high-bandwidth applications, technological advancements and novel applications in the mmWave communication are poised to significantly influence on the evolution of 6G networks [3]. However, mmWave signals suffer severe path loss during transmission as the carrier frequency increases, which is a critical issue for mmWave communications [4]. To address this issue, Massive MIMO systems with large antenna arrays have been introduced to provide directional beams and achieve significant beamforming gain, thereby ensuring sufficient power at the receiver [5]. However, as the number of radio frequency (RF) chains increases, both the hardware cost and power consumption are significantly higher for the conventional MIMO system, which is unaffordable for a dedicated RF chain associated with an antenna in the mmWave Massive MIMO system [6]. To achieve costeffective communication, beamspace Massive MIMO equipped with discrete lens antenna arrays (LAAs) has been regarded as a promising solution. It can provide directional transmission to mitigate path loss with low interference. Furthermore, by selecting a small number of power-focused beams, LAAs can efficiently reduce the number of RF chains and thus reduce the system power [7,8,9]. However, since the number of RF chains is considerably smaller than the number of antennas, the complete channel state information cannot be directly acquired at the baseband [10,11], which is a significant challenge for beamspace Massive MIMO systems.

To reduce the complexity of the beamspace channel estimation, several effective schemes were proposed by utilizing the sparsity inherent of the beamspace domain [12-14]. An estimation scheme based on adaptive support detection was introduced for the beamspace channel in the 3D

mmWave Massive MIMO systems [12]. The image reconstruction algorithm was introduced as a novel estimator to enhance the accuracy of the estimation at low signal-to-noise ratios (SNR) [13]. Furthermore, a channel estimation scheme based on supported detection (SD) was proposed [14], which can provide both reliable performance and lower overhead. However, the schemes are designed for narrowband systems, whereas practical mmWave MIMO systems operate at wideband frequencies to provide high-data rate transmission. Therefore, the existing narrowband channel estimation schemes are not suitable for wideband mmWave communication systems.

Accordingly, several wideband estimation schemes were proposed for beamspace channel estimation [15-19]. A novel approach leveraging the simultaneous orthogonal matching pursuit (SOMP) algorithm was introduced, where the estimation problem was formulated as a multiple measurement vectors (MMV) problem based on the common support, and effectively addressed by the SOMP algorithm [15]. Unfortunately, the assumption of the common support has limited effectiveness in wideband mmWave MIMO systems, where the delay between antennas on the same physical path cannot be ignored due to the large number of antennas and high sampling rate [16]. As a result, the estimated performance is significantly degraded with the common support assumption. To solve this problem, a novel algorithm known as successive support detection (SSD) was proposed for the wideband beamspace channel estimation without assuming common support [17]. In this method, each path component of the wideband beamspace channel exhibits a unique variable-frequency sparse structure, and all sparse path components are successively estimated based on the SSD scheme. Furthermore, several wideband estimation schemes based on Bayesian algorithm were proposed to improve the estimation accuracy and reduce the pilot overhead [18,19]. However, the estimation schemes [15-19] cannot provide satisfactory estimation performance at the low SNR, especially for the high-dimensional beamspace channel.

In recent years, as an effective iterative method for sparse signal recovery, the approximate message passing (AMP) algorithm [20] has been widely employed for various highdimensional sparse reconstruction problems with low computational overhead. Furthermore, with the development of artificial intelligence (AI), more sophisticated AI-based AMP schemes have been proposed for wideband channel estimation to improve the estimation performance [21,22]. A model-driven channel estimation scheme was proposed, which utilizes neural networks to unfold the AMP algorithm. Compared with the conventional AMP algorithm, the deep unfolding-based AMP algorithm can improve the accuracy of the estimation and thus achieve better performance [21]. A model-driven unsupervised learning network was proposed for wideband beamspace channel by image reconstruction to improve the estimation performance [22]. Nevertheless, the schemes [21,22] may exhibit excellent performance in specific channel conditions and environments, whereas they may lack sufficient generalization in other channel environments. Therefore, it is critical to perform a generalization estimation for the wideband beamspace channel with satisfactory estimation performance.

In this paper, the channel estimation for the wideband

beamspace MIMO system is initially formulated as the general 2D image sparse reconstruction problem. Then, we propose a vector AMP (VAMP) scheme to perform image sparse reconstruction. By the VAMP-based scheme, the 2D image is accurately sparse reconstructed from noisy linear measurements, thus effectively solving the channel estimation problem. The effectiveness of the proposed estimation method is verified by the simulation results, as the proposed scheme outperforms existing estimation methods.

2. SYSTEM MODEL

In this section, the wideband beamspace channel is first introduced. Then, considering the beam squint effect, the wideband beamspace channel estimation problem is formulated. Consider an uplink wideband mmWave Massive MIMO-OFDM system operating with time division multiplexing (TDD), as illustrated in Figure 1. The base station (BS), equipped with $N_{\rm RF}$ RF chains and $N_{\rm BS}$ element LAAs, can provide communication for K single-antenna users simultaneously.

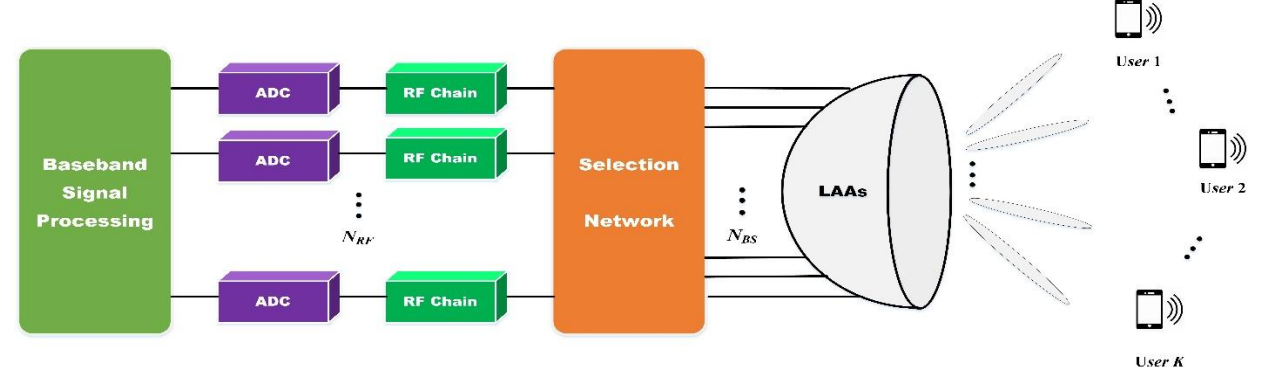


Figure 1. The architecture of the wideband mmWave Massive MIMO-OFDM system equipped with LAAs.

2.1. Wideband Beamspace Channel Model

We apply the classical Saleh-Valenzuela multipath channel model to describe the mmWave Massive MIMO channel model [23]. In the spatial domain, the $N_{BS} \times 1$ channel vector \boldsymbol{h}_m between the BS and the specific user at subcarrier $m(m=1,2,\cdots,M)$ can be expressed as

$$\boldsymbol{h}_{m} = \sqrt{\frac{N_{BS}}{L}} \sum_{l=1}^{L} \zeta_{l} e^{-j2\pi \tau_{l} f_{m}} \boldsymbol{\alpha}(\phi_{l,m}), \qquad (1)$$

where the number of resolvable channel paths, the time delay of the $\ ^l$ -th path, and the complex gain of the $\ ^l$ -th path are defined as $\ ^L$, $\ ^{\tau_l}$ and $\ ^{\zeta_l}$, respectively. Then, $\ ^{\phi_{l,m}}$ represents the spatial direction at subcarrier $\ ^m$ and can be expressed as

$$\phi_{l,m} = \frac{f_m}{c} d \sin \theta_l, \qquad (2)$$

where c is the light speed, and $s_l \in [-\pi/2, \pi/2]$ is the physical direction. Furthermore, s_m represents the frequency of the subcarrier s_m in the wideband mmWave Massive MIMO-OFDM system, and can be expressed as

$$f_m = f_c + \frac{f_s}{M} \left(m - 1 - \frac{M - 1}{2} \right),$$
 (3)

where the sampling rate and the carrier frequency are defined as f_s and f_c , respectively. The antenna spacing is given by $d=c/2f_c$. Notably, $\phi_{l,m}$ is frequency-independent in the narrowband mmWave system, whereas $\phi_{l,m}$ is frequency-dependent in the wideband mmWave system [24]. Furthermore, $\alpha(\phi_{l,m})$ is the array steering vector in term of the spatial direction $\phi_{l,m}$. For the typical N_{BS} -element uniform linear array (ULA), $\alpha(\phi_{l,m})$ can be defined as

$$\alpha(\phi_{l,m}) = \frac{1}{\sqrt{N_{BS}}} [e^{-j2\pi\phi_{l,m}i}]_{i \in I(n)}, \tag{4}$$

where
$$I(n) = \left[-\frac{N_{BS} - 1}{2}, -\frac{N_{BS} - 3}{2}, \dots, \frac{N_{BS} - 1}{2} \right]^T$$
 is the

symmetrical number set centered at the zero.

By exploiting the LAAs, the wideband mmWave MIMO channel in the spatial domain is transformed into the beamspace representation. Notably, the LAAs essentially fulfil the role of the spatial Fourier transform, and the wideband beamspace channel vector $\bar{\boldsymbol{h}}_m$ can be expressed as

$$\bar{h}_{m} = F_{bsp} h_{m} = F_{bsp} \sqrt{\frac{N_{BS}}{L}} \sum_{l=1}^{L} \zeta_{l} e^{-j2\pi\tau_{l} f_{m}} \alpha(\phi_{l,m}) = \sqrt{\frac{N_{BS}}{L}} \sum_{l=1}^{L} \zeta_{l} e^{-j2\pi\tau_{l} f_{m}} \bar{b}_{l,m}. \tag{5}$$

The F_{bsp} contains N_{BS} orthogonal array steering vectors that are associated with the N_{BS} beam directions over the whole physical space, and can be presented as

$$\boldsymbol{F}_{bsp} = [\boldsymbol{\alpha}(\overline{\phi}_1), \boldsymbol{\alpha}(\overline{\phi}_2), \cdots, \boldsymbol{\alpha}(\overline{\phi}_{N_{ps}})]^H, \tag{6}$$

where
$$\overline{\phi}_{n} = \frac{1}{N_{BS}} \left(n - \frac{N_{BS} + 1}{2} \right), n = 1, 2, ..., N_{BS}$$
 is the

spatial direction predefined by the LAAs. $\bar{b}_{l,m}$ stands for the l-th component at subcarrier m in the beamspace domain, and can be defined as

$$\overline{\boldsymbol{b}}_{l,m} = \boldsymbol{F}_{bsp} \boldsymbol{\alpha} \left(\phi_{l,m} \right) = \left[\Theta \left(\phi_{l,m} - \overline{\phi}_{l} \right), \dots, \Theta \left(\phi_{l,m} - \overline{\phi}_{N_{BS}} \right) \right]^{T},$$
where $\Theta(x) \triangleq \frac{\sin N2\pi x}{\sin \pi x}$ is the Dirichlet function. Due to

the power-focused property of the $\Theta(x)$ function, the majority power of $\overline{b}_{l,m}$ is concentrated on a limited number of directions. Moreover, the number of resolvable paths is typically small since there is limited scattering in the mmWave communication. Therefore, the wideband beamspace channel \overline{h}_m is a sparse vector. However, different from narrowband mmWave systems, the spatial direction $\phi_{l,m}$ in the wideband mmWave systems is frequency-dependent, which is due to the well-known beam squint [25]. Considering the beam squint effect, the assumption of the common support for the wideband beamspace channel is no longer valid. Although the wideband beamspace channel has the sparse structure, existing estimation schemes with the common support assumption suffer significant performance degradation.

2.2. Problem Formulation

If the channel remains unchanged during each symbol period in the uplink TDD system, the pilot signals are transmitted to the BS for the channel estimation. We employ the orthogonal pilot scheme to perform channel estimation for each user individually [26]. Without loss of generality, considering a given user in the wideband mmWave Massive MIMO-OFDM system, we define $P_{m,n}$ as the pilot transmitted in instant n at the subcarrier m. The $N_{RF} \times 1$ received pilot signals $\mathbf{r}_{m,n}$ can be expressed as

$$\mathbf{r}_{m,n} = \mathbf{A}_n \overline{\mathbf{h}}_m p_{m,n} + \mathbf{A}_n \mathbf{n}_{m,n}, \quad m = 1, 2, \dots, M,$$
 (8)

where A_n and $n_{m,n} \sim \mathcal{CN}\left(0,\sigma^2 I_N\right)$ are defined as the $N_{RF} \times N_{BS}$ hybrid combining matrix and the $N_{BS} \times 1$ noise vector with σ^2 representing the noise power, respectively. Considering \$N\$ instants of the transmitted pilot signals and letting $p_{m,n} = 1$ for n = 1, ..., N, the overall received pilot signal $\overline{r}_m = \begin{bmatrix} r_{m,1}^T, r_{m,2}^T, \cdots, r_{m,N}^T \end{bmatrix}^T$ at the m-th subcarrier can be expressed as

$$\bar{\mathbf{r}}_{m} = \bar{\mathbf{A}}\bar{\mathbf{h}}_{m} + \bar{\mathbf{n}}_{m}, \quad m = 1, 2, \dots, M,$$
(9)

where $\overline{\mathbf{n}}_{m}$ represents the effective noise vector, $\overline{\mathbf{A}} = \begin{bmatrix} \mathbf{A}_{1}^{T}, \mathbf{A}_{2}^{T}, \cdots, \mathbf{A}_{N}^{T} \end{bmatrix}^{T}$ is the hybrid combining matrix of size $NN_{RF} \times N_{BS}$. The elements of $\overline{\mathbf{A}}$ are randomly selected from the set $\left\{ -\frac{1}{\sqrt{NN_{RE}}}, +\frac{1}{\sqrt{NN_{RE}}} \right\}$ with equal probability.

Notably, while the beamspace channel vectors of different subcarriers may be different due to beam squint effects, they are still correlated with the array response vectors [27]. Considering this, the channel estimation can be viewed as the 2D image sparse reconstruction problem, where several sparse reconstruction algorithms are utilized to perform the channel estimation.

3. VAMP-BASED CHANNEL ESTIMATION

In this section, we firstly review the AMP algorithm. Then, by leveraging the VAMP-based scheme, 2D natural image is accurately sparse reconstructed, which effectively solves the beamspace channel estimation problem.

3.1. AMP Algorithm

As a powerful iterative method for sparse signal recovery, the AMP algorithm has been widely employed for the high-dimensional sparse channel estimation with low computational complexity. In wideband mmWave Massive MIMO systems, there is a significant increase in the number of antennas compared to traditional MIMO systems. Thus, the dimension of the sparse signal in (5) is high. Since the AMP algorithm has the fast convergence, and low computational complexity, which make it as the efficient estimation scheme for high-dimensional channel estimation. The beamspace channel estimation scheme based on the AMP algorithm [28] is demonstrated in Algorithm 1.

In Algorithm 1, the key stage of the AMP estimation scheme is step 4, where the estimate \bar{h}_{t+1} in the t-th iteration is obtained via the shrinkage function η_{st} and can be defined as

```
Algorithm 1: The AMP-based wideband beamspace channel estimation scheme Input: The received signal vector \overline{\mathbf{r}}, the combining matrix \overline{\mathbf{A}}, the number of iterations T. Initialization: \mathbf{v}_{-1} = \mathbf{0}, b_0 = 0, c_0 = 0, \tilde{\mathbf{h}}_0 = \mathbf{0}. for t = 0, 1, \dots, T - 1 do

1. \mathbf{v}_t = \overline{\mathbf{r}} - \overline{\mathbf{A}} \hat{\mathbf{h}}_t + b_t \mathbf{v}_{t-1} + c_t \mathbf{v}_{t-1}^*
2. \sigma_t^2 = \frac{1}{M} \|\mathbf{v}_t\|_2^2
3. \mathbf{r}_t = \hat{\mathbf{h}}_t + A^T \mathbf{v}_t
4. \hat{\mathbf{h}}_{t+1} = \mathbf{h}_{bt}(\mathbf{r}_t; \lambda_t, \sigma_t^2)
5. b_{t+1} = \frac{1}{M} \sum_{i=1}^{N} \frac{\partial g_{ta}(\mathbf{r}_{t,i}; \lambda_t, \sigma_t^2)}{\partial \mathbf{r}_{t,i}}
6. c_{t+1} = \frac{1}{M} \sum_{i=1}^{N} \frac{\partial g_{ta}(\mathbf{r}_{t,i}; \lambda_t, \sigma_t^2)}{\partial \overline{\mathbf{r}}_{t,i}}
end for Output: Sparse signal recovery results: \hat{\mathbf{h}} = \hat{\mathbf{h}}_{tr}.
```

$$\bar{\boldsymbol{h}}_{t+1} = \eta_{st}(\boldsymbol{r}_t; \lambda_t, \sigma_t^2), \tag{10}$$

$$\left[\eta_{st}\left(\mathbf{r}_{t};\lambda_{t},\sigma_{t}^{2}\right)\right]_{i} = \eta_{st}\left(\left|\mathbf{r}_{t,i}\right|e^{j\omega_{t,i}};\lambda_{t},\sigma_{t}^{2}\right) = \max\left(\left|\mathbf{r}_{t,i}\right| - \lambda_{t}\sigma_{t},0\right)e^{j\omega_{t,i}},\quad(11)$$

where $\omega_{t,i}$ stands for the phase of complex-valued element $r_{t,i}$ and σ_t^2 is updated by estimating the noise variance. Furthermore, λ_t is the fixed and predefined parameter in the t-th iteration. While the AMP estimation scheme has shown excellent performance in dealing with large-scale sparse signal recovery problems, there is still a critical issue when it is employed for beamspace channel estimation. Since the shrinkage parameter λ_t usually employs the same empirical value in all iterations, it tends to requires several experiments to obtain a satisfactory value. In addition, the AMP algorithm may fail to converge when the sensing matrix is beyond independent identical distributed (IID) sub-Gaussian region.

3.2. VAMP-based wideband beamspace channel estimation

Vector AMP (VAMP) is a computationally efficient iterative algorithm designed to enhance the performance in the standard linear regression problem [29]. As an extension and enhancement of the AMP, the VAMP algorithm is particularly suitable for where the transform matrix does not have IID Gaussian entries, or when the matrix is ill-conditioned. The main insight of the VAMP algorithm is derived from the consideration of the singular value decomposition (SVD) for the transformation matrix. Specifically, consider the economic SVD of $A \in \mathbb{R}^{M \times N}$

$$\mathbf{A} = \mathbf{U} \operatorname{Diag}(\mathbf{s}) \mathbf{V}^{T}, \tag{12}$$

where $s \in \mathbb{R}^R$ with $R = \operatorname{rank}(A) \le \min(M, N)$ and s contains the positive singular values of A. For the transformation matrix A, the matrix V will contain the first R columns of a matrix which is uniformly distributed on the group of $N \times N$ orthogonal matrices. Note that VAMP performs well for any singular value s and any orthogonal matrix s and s are sufficiently large [30].

Consider the linear inverse problem of the linear inverse problem \bar{h}_m from noisy linear measurements of (9). VAMP provides the same benefits as AMP, but for a wider variety of matrices. With the powerful application range and excellent recovery performance of the VAMP, the VAMP-based wideband beamspace channel estimation scheme is proposed, as shown in Algorithm 2.

The VAMP estimation scheme is described in Algorithm 2, and more detailed information about the VAMP algorithm can be accessed [29]. $g^{(*,\gamma_t)}$ is a separable Lipschitz denoising function parameterized by γ_t . f_t is the true signal \bar{h}_0 with Gaussian white noise, and can be expressed as

Algorithm 2: The VAMP-based wideband beamspace than the combining matrix $\tilde{\mathbf{A}} \in \mathbb{R}^{NN_{RF} \times N_{RS}}$, denoiser $\mathbf{g}(\cdot, \gamma_t)$, the noise variance σ^2 , and the number of iterations T.

Initialization: Set h_0 to 0 and $\gamma_0 \geq 0$. Compute economy SVD $\mathbf{A} = \mathbf{U} \mathrm{Diag}(\mathbf{s}) \mathbf{V}^T$ with $\mathbf{V}^T \mathbf{V} = \mathbf{I}_R$, $\mathbf{U}^T \mathbf{U} = \mathbf{I}_R$, se $\mathbb{R}^R_+ R = \mathrm{rank}(\mathbf{A})$. Compute preconditioned $\tilde{\mathbf{r}} := \mathrm{Diag}(\mathbf{s})^{-1} \mathbf{U}^T \mathbf{F}$.

for $t = 0, 1, \cdots, T - 1$ do

1. $\tilde{\mathbf{h}}_t = \mathbf{g}(\mathbf{f}_t, \gamma_t)$ 2. $\alpha_t = (\mathbf{g}^t(\mathbf{f}_t, \gamma_t))$ 3. $\tilde{\mathbf{t}}_t = (\mathbf{h}_t - \alpha_t \mathbf{f}_t)/(1 - \alpha_t)$ 4. $\tilde{\gamma}_t = \gamma_t (1 - \alpha_t)/\alpha_t$ 5. $\mathbf{b}_t = \frac{1}{\sigma^t} \mathrm{Diag}(\frac{1}{\sigma^t} \mathbf{F}^2 + \tilde{\gamma}_t \mathbf{1})^{-1} \mathbf{s}^2$ 6. $\gamma_{t+1} = \tilde{\gamma}_t (\mathbf{b}_t)/(\frac{N_t^2}{R^2} - (\mathbf{b}_t))$ 7. $\mathbf{f}_{t+1} = \tilde{\mathbf{f}}_t + \frac{N_t^2}{R^2} \mathrm{VDiag}(\mathbf{b}_k/(\mathbf{b}_t)) \left(\tilde{\mathbf{f}} - \mathbf{V}^T \tilde{\mathbf{f}}_t\right)$ end for Output: Sparse signal recovery results: $\tilde{\mathbf{h}} = \hat{\mathbf{h}}_T$.

$$f_{t} = \overline{h}_{0} + \mathcal{N}(\boldsymbol{0}, \sigma^{2}\boldsymbol{I})$$
 (13)

 $\langle {m g}'(f_t,\gamma_t)
angle$ is its divergence at f_t . Specifically, ${m g}'(f_t,\gamma_t)$ is the diagonal of the Jacobian

$$g(f_t, \gamma_t) = \operatorname{diag}\left[\frac{\partial g(f_t, \gamma_t)}{\partial f_t}\right],$$
 (14)

and $\langle \cdot \rangle$ is the empirical averaging operation

$$\langle \boldsymbol{d} \rangle := \frac{1}{N} \sum_{n=1}^{N} d_n. \tag{15}$$

In line 5, s^2 is the square component of vector s.

4. SIMULATION RESULTS

In this section, a typical wideband mmWave Massive MIMO-OFDM system is considered, where the BS is

equipped with $N_{BS}=256$ LAAs antennas and $N_{RF}=16$ RF chains to provide communication with K=16 users simultaneously. The total number of subcarriers is set at M=128. In addition, the system bandwidth and carrier frequency are $f_s=4G$ and $f_c=28G$, respectively. The spatial channel parameters for each user is defined as follows [17]. Finally, we define SNR for the channel estimation as a key parameter, which is denoted by the value of $1/\sigma^2$. The performance of channel estimation can be evaluated by the normalized mean square error (NMSE), and is given as

NMSE =
$$\frac{\mathbb{E}\left\{\sum_{t=1}^{T} \left\| \overline{\boldsymbol{h}}_{t} - \overline{\boldsymbol{h}}_{t} \right\|_{2}^{2} \right\}}{\mathbb{E}\left\{\sum_{t=1}^{T} \left\| \overline{\boldsymbol{h}}_{t} \right\|_{2}^{2} \right\}},$$
 (16)

where \bar{h}_t is an estimate of the genuine channel vectors \bar{h}_t . Figure 2 illustrates the NMSE performance comparative analysis with different estimation schemes by employing the ULA array structure at different SNRs. The comparative evaluation reveals that the proposed VAMP-scheme achieves low NMSE over the examined SNRs range, thereby eclipsing the performance of the three existing schemes. A detailed examination of the results shows that the NMSE performance of the OMP and AMP algorithms is significantly below the optimal level. On the contrary, the proposed approach significantly improves the NMSE performance.

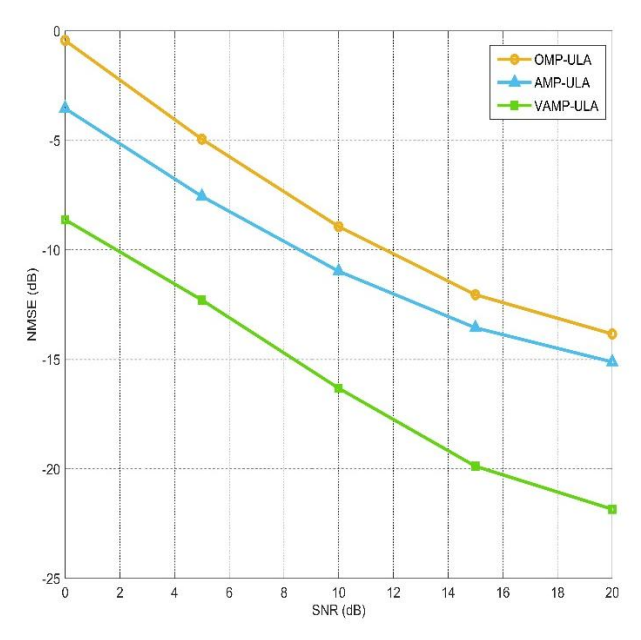


Figure 2. The NMSE performance comparison for ULA arrays with different estimation schemes

In addition to evaluating the NMSE performance of ULA, we also investigate different channel estimation schemes with UPA array structure. Figure 3 provides the comparison of the NMSE performance with different schemes based on the 16×16 UPA array. It can be noticed that the conventional OMP algorithm and the AMP algorithm cannot provide satisfactory estimation performance. On the contrary, the proposed VAMP-scheme still outperforms the other three schemes, which further verifies the effectiveness of the proposed scheme.

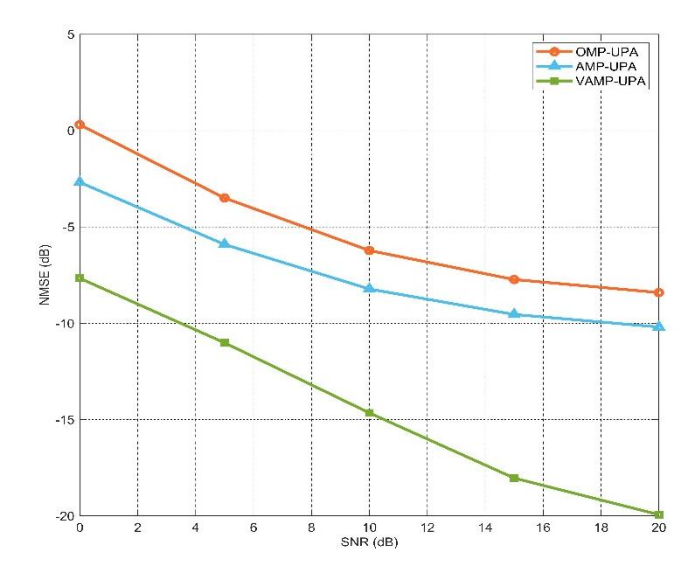


Figure 3. The NMSE performance comparison for UPA arrays with different estimation schemes

5. Conclusion

In this paper, we propose a VAMP-based scheme to solve the wideband beamspace channel estimation problem. Specifically, the beamspace channel estimation is formulated as the 2D image sparse reconstruction problem. Subsequently, by utilizing the VAMP-based scheme, the wideband beamspace channel estimation problem is effectively addressed. Simulation results validate the effectiveness of the proposed method and highlight its superior performance against other estimation schemes.

References

- [1] M. Xiao, S. Mumtaz, Y. Huang, L. Dai, Y. Li, M. Matthaiou, G. K. Karagiannidis, E. Bj"ornson, K. Yang, I.Chih-Lin, et al., "Millimeter wave communications for future mobile networks," IEEE Journal on SelectedAreas in Communications, vol. 35, no. 9, pp. 1909–1935, (2017)
- [2] A. L. Swindlehurst, E. Ayanoglu, P. Heydari, and F. Capolino, "Millimeter-wave Massive MIMO: The next wireless revolution?," IEEE Communications Magazine, vol. 52, no. 9, pp. 56–62, (2014)
- [3] X.-H. You, C.-X. Wang, J. Huang, X. Gao, Z. Zhang, M. Wang, Y. Huang, C. Zhang, etal., "Towards 6g wireless communication networks: Vision, enabling technologies, and new paradigm shifts," Science China Information Sciences, vol. 64, pp. 1–74, (2021)
- [4] T. S. Rappaport, S. Sun, R. Mayzus, H. Zhao, Y. Azar, K. Wang, G. N. Wong, J. K. Schulz, M. Samimi, and F. Gutierrez, "Millimeter wave mobile communications for 5g cellular: It will work!," IEEE Access, vol.1, pp. 335–349, (2013)
- [5] L. Wei, R. Q. Hu, Y. Qian, and G. Wu, "Key elements to enable millimeter wave communications for 5g wireless systems," IEEE Wireless Communications, vol. 21, no. 6, pp. 136–143, (2014)
- [6] X. Gao, L. Dai, S. Han, I. Chih-Lin, and R. W. Heath, "Energy-efficient hybrid analog and digital precoding for mmwave mimo systems with large antenna arrays," IEEE Journal on Selected Areas in Communications, vol. 34, no. 4, pp. 998–1009, (2016)
- [7] J. Brady, N. Behdad, and A. M. Sayeed, "Beamspace mimo for millimeter-wave communications: System architecture, modeling, analysis, and measurements," IEEE Transactions on Antennas and Propagation, vol. 61, no. 7, pp. 3814–3827, (2013)

- [8] Y. Zeng, R. Zhang, and Z. N. Chen, "Electromagnetic lensfocusing an-tenna enabled Massive mimo: Performance improvement and cost reduc-tion," IEEE Journal on Selected Areas in Communications, vol. 32, no. 6, pp. 1194–1206, (2014)
- [9] O. Quevedo-Teruel, M. Ebrahimpouri, and F. Ghasemifard, "Lens anten-nas for 5g communications systems," IEEE Communications Magazine, vol. 56, no. 7, pp. 36–41, (2018)
- [10] Y. Zeng and R. Zhang, "Millimeter wave mimo with lens antenna array: A new path division multiplexing paradigm," IEEE Transactions on Communications, vol. 64, no. 4, pp. 1557–1571, (2016)
- [11] A. Sayeed and J. Brady, "Beamspace mimo for highdimensional multiuser communication at millimeter-wave frequencies," in 2013 IEEE global communications conference (GLOBECOM), pp. 3679–3684, IEEE, (2013)
- [12] X. Gao, L. Dai, S. Han, I. Chih-Lin, and F. Adachi, "Beamspace channel estimation for 3D lens-based millimeterwave Massive mimo systems," in 2016 International Conference on Wireless Communications & Signal Processing (WCSP), pp. 1–5, IEEE, (2016)
- [13] J. Yang, C.-K. Wen, S. Jin, and F. Gao, "Beamspace channel estimation in mmwave systems via cosparse image reconstruction technique," IEEE Transactions on Communications, vol. 66, no. 10, pp. 4767–4782, (2018)
- [14] X. Gao, L. Dai, S. Han, I. Chih-Lin, and X. Wang, "Reliable beamspace channel estimation for millimeter-wave Massive mimo systems with lens antenna array," IEEE Transactions on Wireless Communications, vol. 16, no. 9, pp. 6010–6021, (2017)
- [15] Z. Gao, C. Hu, L. Dai, and Z. Wang, "Channel estimation for millimeterwave Massive MIMO with hybrid precoding over frequency-selective fading channels," IEEE Communications Letters, vol. 20, no. 6, pp.1259–1262, (2016)
- [16] B. Wang, F. Gao, S. Jin, H. Lin, and G. Y. Li, "Spatial-and frequency wideband effects in millimeter-wave Massive MIMO systems," IEEE Transactions on Signal Processing, vol.66, no.13, pp. 3393–3406, (2018)
- [17] X. Gao, L. Dai, S. Zhou, A. M. Sayeed, and L. Hanzo, "Wideband beamspace channel estimation for millimeter-wave mimo systems relying on lens antenna arrays," IEEE Transactions on Signal Processing, vol. 67, no. 18, pp.4809– 4824, (2019)
- [18] X. Cheng, J. Deng, and S. Li, "Wideband Channel Estimation for Millimeter Wave Beamspace MIMO," IEEE Transactions on Vehicular Technology, vol. 70, no. 7, pp. 7221–7225, (2021)
- [19] X. Mo, W. Ma, L. Gui, L. Zhang, and X. Sang, "Beamspace Channel Estimation With Beam Squint Effectfor the Millimeter-Wave MIMO-OFDM Systems," IEEE Access, vol. 9, pp. 153037–153049, (2021)
- [20] D. L. Donoho, A. Maleki and A. Montanari, "Message passing algorithms for compressed sensing: I. Motivation and construction," in 2010 IEEE Inf. Theory Workshop (ITW Cairo), pp. 1–5, IEEE, (2010)
- [21] He, H., Wen, C.K., Jin, S., Li, G.Y, "Deep learning-based channel estimation for beamspace mmwave Massive mimo systems," IEEE Wireless Communications Letters vol.7, no.5, pp.852–855, (2018)
- [22] H. He, R. Wang, W. Jin, S. Jin, C. -K. Wen and G. Y. Li, "Beamspace Channel Estimation for Wideband Millimeter-Wave MIMO: A Model-Driven Unsupervised Learning Approach," IEEE Transactions on Wireless Communications, vol. 22, no. 3, pp. 1808-1822, (2023)
- [23] R. W. Heath, N. Gonzalez-Prelcic, S. Rangan, W. Roh, and A. M. Sayeed, "An overview of signal processing techniques for

- millimeter wave mimo systems," IEEE journal of selected topics in signal processing, vol. 10, no. 3, pp. 436–453, (2016)
- [24] X. Gao, L. Dai, S. Zhou, A. M. Sayeed, and L. Hanzo, "Beamspace channel estimation for wideband millimeter-wave mimo with lens antenna array," in 2018 IEEE International Conference on Communications (ICC), pp. 1–6, IEEE, (2018)
- [25] B. Wang, F. Gao, G. Y. Li, S. Jin, and H. Lin, "Wideband channel estimation for mmwave Massive mimo systems with beam squint effect," in 2018 IEEE Global Communications Conference (GLOBECOM), pp.1–6, IEEE, (2018)
- [26] Y. Nie, "Deterministic Pilot Pattern Placement Optimization for OFDM Sparse Channel Estimation," IEEE Access, vol. 8, pp. 124783–124791, (2020)

- [27] H. He, C. -K. Wen, S. Jin and G. Y. Li, "Model-Driven Deep Learning for MIMO Detection," IEEE Transactions on Signal Processing, vol. 68, pp. 1702–1715, (2020)
- [28] X. Wei, C. Hu and L. Dai, "Deep Learning for Beamspace Channel Estimation in Millimeter-Wave Massive MIMO Systems," IEEE Transactions on Communications, vol. 69, no. 1, pp. 182–193, (2021)
- [29] S. Rangan, P. Schniter and A. K. Fletcher, "Vector Approximate Message Passing," IEEE Transactions on Information Theory, vol. 65, no. 10, pp. 6664–6684, (2019)
- [30] M. Borgerding, P. Schniter and S. Rangan, "AMP-Inspired Deep Networks for Sparse Linear Inverse Prob-lems," IEEE Transactions on Signal Processing, vol. 65, no. 16, pp. 4293– 4308, (2017)